

*Research article*

## Improved methods for controlling interconnected DC microgrids in rural villages

Pascal Hategekimana<sup>1</sup>, Adrià Junyent-Ferré<sup>2</sup>, Etienne Ntagwirumugara<sup>1</sup> and Joan Marc Rodriguez Bernuz<sup>3</sup>

<sup>1</sup> African Center of Excellence Energy for Sustainable Development, College of Science and Technology, University of Rwanda (ACEESD, CST-UR), Po Box 3900- Kigali-Rwanda

<sup>2</sup> Electrical and Electronics Engineering Department, Imperial College London, UK

<sup>3</sup> Department of Electrical Engineering, Universitat Politècnica de Catalunya, Spain

\* **Correspondence:** Email: hategekapascal@gmail.com; Tel: +250729055208.

**Abstract:** Interconnected Microgrid (IMG) networks have been suggested as the best to build electrical networks in remote villages far from the main electricity grid by interconnecting the nearby distributed energy resources (DERs) through power electronic converters. Interconnecting different DERs results in voltage deviation with unequal power-sharing, while voltage performance is a significant challenge. The control strategies for these converters are essential in the operational stability of any IMG network under study. In this paper, we propose an improved droop control method aiming to manage the power flow among the IMGs by maintaining the constant desired voltages in the network with minimum voltage deviation, resulting in the minimization of power losses. We found that the minimum voltage deviation at the load side (converter-3) was between 0.58 and 0.56 V, while the voltage deviation for both converter-1 and converter-2 remained below 0.5 V. This leads to efficient voltage regulation, resulting in the stability of an IMG network. To verify the feasibility of this method, MATLAB/SIMULINK has been used.

**Keywords:** droop controllers; microgrid; circulating current; load-sharing; voltage regulation

---

### 1. Introduction

For many years, the national power grid was the only way the electrical power generated from

large-scale power plants could be transmitted and distributed at long distances reaching industrial, business, or domestic sites, which induced high material costs and single power line dependency [1]. Recently, low-voltage microgrids (LVMG) have become a crucial solution, especially in rural villages where national grid power cannot be reached. Microgrid is presented as the means to produce power from sustainable energy sources near the consumption sites, and once these distributed energy resources (DERs) are connected to form a cluster of interconnected microgrid (IMG) networks, its energy control necessitates a specified control operation [2] for ensuring reliability and comfort to the power consumers. Compared to the individual MG, a network of IMGs has additional control flexibilities for satisfying the necessities of a grid network with the following advantages: (i) To improve the grid reliability, i.e., it can recover its operation suddenly under the grid disturbance; (ii) to maximize the DERs utilization; (iii) to improve the daily power quality to the grid residential and improve their living standards in the remote regions; and finally, (iv) to improve load demand [1]. In this paper, this network of IMG for the case study is concerned with the interconnection of individual solar PV off-grid for maintaining the availability of electricity among different power consumers [3], and the analysis of specified control strategy was discussed here.

In previous works, it was found that when using conventional droop control, it will not be possible to achieve power-sharing among the DERS due to voltage deviation caused by the different line impedances in the IMG [1]. Thus, a DC microgrid (DCMG) is considered an efficient, reliable, and scalable solution to electrify remote areas, needing a consistent control scheme like hierarchical control [4,5]. From this hierarchical control, the droop control method was achieved by adding internal or external resistance (s) in the parallel connected converters of the IMG to maintain proper current sharing. The droop control is a mechanism employed in power generators for sharing the load between DERs that are interconnected in the networks. The implementation of this method is not complicated because it does not necessitate line communication systems. Applying the droop control method, it is important to consider the following two major parameters: (I) Voltage control, ensuring the voltage regulation in the IMG, and (II) Current control, providing identical current sharing among the network converters [6]. Without droop control, the connection of DERs under fixed output voltage control leads to improper power-sharing due to the differences in line resistance [1]. Numerous droop control schemes were proposed for achieving power-sharing among converters in the IMGs [7].

In this paper, an improved droop control method for controlling an IMG with different DC sources in a remote area where the power sources are from solar PV was analyzed. There exist several DCMG control issues, including voltage regulation between parallel converters, current sharing, maximum power point tracking, etc... [8]. In [6], it was found that the conventional droop control suffered from poor voltage regulation and unequal load sharing among converters when the voltage sources are unequal due to load demand variations [9]. The voltage regulation and load sharing in DCMGs are crucial operations to be implied for maintaining a near-constant output voltage in the IMG network under different loading conditions [8], and in this paper, an improved method to manage proper load sharing with minimum voltage deviation was used.

Our major objectives of this paper were to ensure the control strategy with minimization of voltage deviation between the reference voltage and the desired output voltage, providing a proper load sharing with a reduced circulating current and power loss. This method has also been used to ensure the stability and performance of IMG systems in remote areas. Apart from the introduction section, the rest of the paper is also organized as follows: Section 2 discusses an overview of DC microgrid systems and their controls. Section 3 is concerned with the modelling and analysis of the proposed network with the droop control method. Section 4 represents the methodology used to achieve the results of this work, Section 5 discusses the results, and finally, section 6 is the conclusion of this paper.

## 2. Interconnected microgrid structures

The three most common types of MGs depending on the power type include: i) DC microgrids (DCMGs), ii) AC microgrids (ACMGs), and iii) hybrid AC and DCMGs [10]. Although DCMGs are less common today, it is believed that they have the potential to increase efficiency by reducing switching levels in the network [11]. They are also easier to control than ACMG when reactive power control is required [12]. Figure 1 shows a typical DCMG network which includes energy sources such as solar PV, fuel cells, and wind to supply DC loads is shown in Figure 1, where the generated AC power is integrated into the DCMG system through appropriate power converters [13].

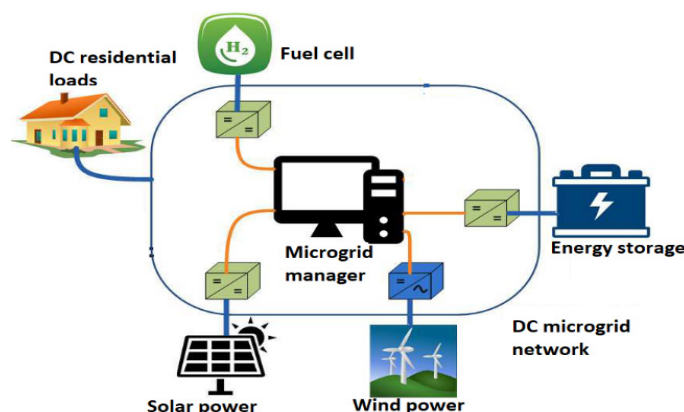


**Figure 1.** Typical DC microgrid with sources and load [4], modified.

Furthermore, electric vehicles (EVs), data centres, telecommunication stations, and most electronic devices in DC form (lamps, phones, computers, etc.) do not necessitate power conversion stages when used in DCMG, which improves the system efficiency [12]. Thus, referring to the case study in this paper, individual solar PV sources cannot afford the power demand in the village of Bugesera district (Eastern province) [3], where the electrical (domestic) loads are, radios, TVs, and phone charging points, while loads with high voltage including milling machines, welding machines are not supported by this method of power generation. Nowadays, the growth in power semiconductor devices has made DC power efficient and popular, through the expansion of existing individual off-grid power sources to the MGs [14]. To maximize the utilization of the power generated from different MGs and at the same time improve its reliability and efficiency, flexible control strategies are needed [15], where different MGs are also combined to formulate a cluster of IMG [16]. Figure 2 shows an IMG with the power lines of resistances  $R_C$  connecting individual MGs to the main bus [17].

In this paper, our main purpose is to deliver communal power-sharing between neighboring MGs, resulting in MG reliability and operational cost reduction [18]. The converters are used to provide the needed voltage in the main DC bus depending upon the load demand. On one side, the main advantages of an IMG are: (i) Boosting renewable energy penetration, (ii) improving the MG dependability and stability; (iii) enhancing operational system efficiency, and economy [11]; and (iv) mutual assistance between each MG during generation deficiency in the network as an alternative way of importing power from the main grid [12]. From the above advantages, it can be noted that, the formulation of IMG in this study can recover the shortage of all possible load demand, resulting in the economic and health development of the people in the village.

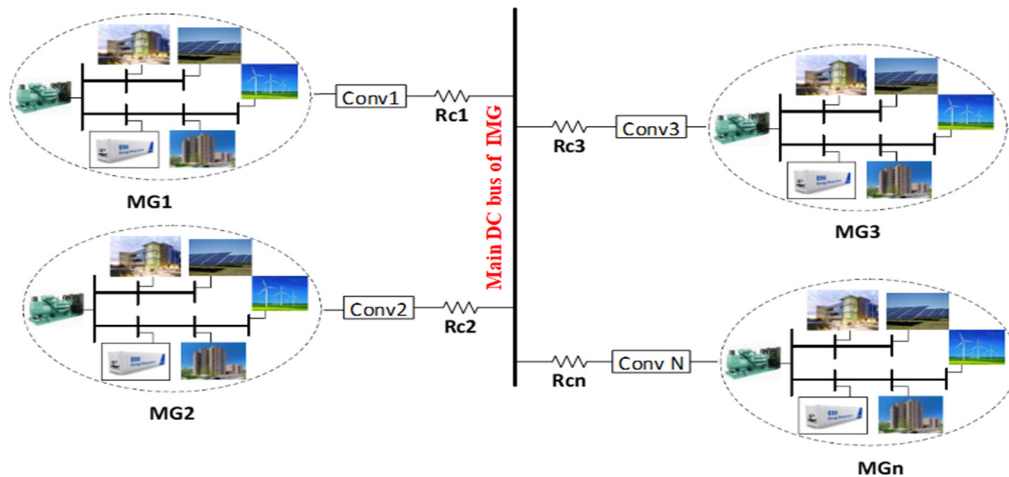


**Figure 2.** Proposed IMG model with n-MG.

On the other side, IMG may face the following challenges: (1) Lack of standardization of system communications and components, (2) Power flow control issues to maintain grid stability by balancing power generation and consumption, (3) Grid synchronization when connected to the main AC grid [19], and (4) Special protection mechanisms are required to prevent faults and ensure the safety of personnel working on DC systems [17]. Referring to the above-mentioned challenges, the correct selection of any IMG installation should be considered based on the availability of energy resources, load demands, and the control method used. According to the network topologies, DCMGs are classified into three types: (i) Star (radial), (ii) ring-main, and (iii) mesh systems [20], and ring-main topology was found to provide more advantages over others.

### 2.1. Control strategies of DC microgrid clusters

There are different methods used to control an IMG system [10]. The four categories of control strategies comprise (i) hierarchical control, (ii) distributed, (iii) centralized, and (iv) decentralized methods [21]. Referring to [9], a hierarchical controller can enhance the performance of the primary controller for dynamically managing the voltage and power in the IMGs.

### 2.2. Hierarchical control

This hierarchical control can be structured in three levels of hierarchy: (1) Primary, (2) secondary, and (3) tertiary [22] as shown in Figure 3. This hierarchical control permits the efficient control operation of an IMG [4]. Referring to [23] and using Figure 3, the primary control method is concerned with voltage stability improvement, power and current sharing, virtual impedance control, and droop control. The secondary control is concerned with the error correction in current and voltage, linked to the power-sharing from the IMG [9,24]. In this paper, the droop control method from primary control was analysed due to its efficiency and flexibility in the IMG control.

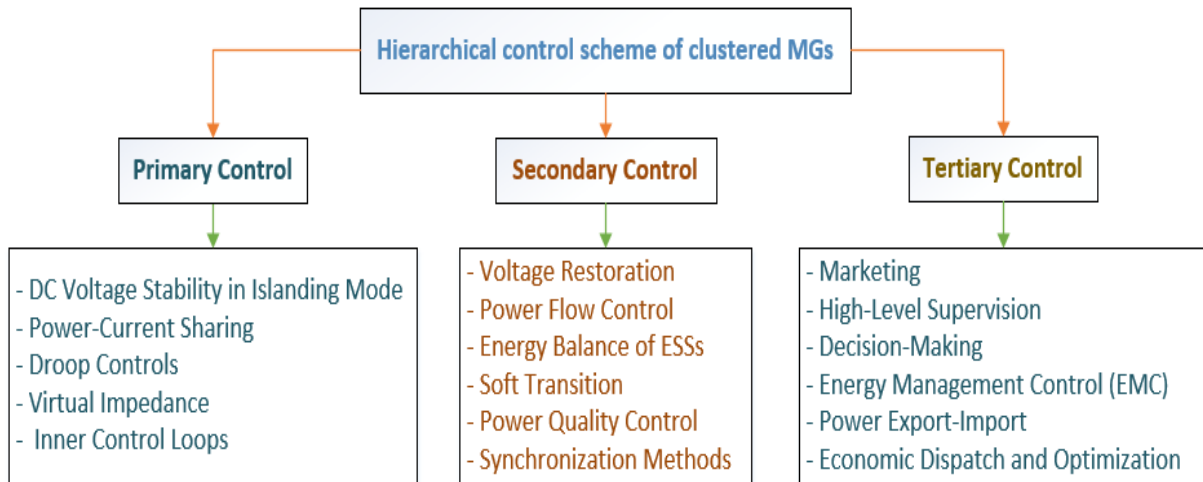


**Figure 3.** Hierarchical control scheme of an interconnected DCMG [24], modified.

It was noted that tertiary control deals with energy and power management, which results in the minimization of operational costs and power loss in the DCMG system [22]. It has been reported from the three aforementioned control methods that the accuracy of current sharing was degraded resulting from the voltage drop across the respective line impedance. Thus, the current sharing in DCMG can be realized using current and voltage droop gain controllers ( $K_{1,2,...,n}$ ) depending on the network structure, and this can be implemented using a virtual resistance [25]. In this paper, the variation of different values of the K-controllers was analysed to assess the feasibility of this control method.

### 3. Modelling and analysis of the droop control

Droop control was considered the control strategy applied in DCMGs for regulating the power-sharing among different DERs for maintaining the grid network stability [26]. Using droop control, each power source (converter or generator) operates at a fixed impedance, where the output voltage will be related to the corresponding output power. This implies that the increase in load will be followed by the decrease in voltage, and vice versa [26], and this droop control method was used for obtaining current sharing among parallel-connected converters. The droop control technique is also identified as a primary control technique operating without a communication network for proper power-sharing, lower cost, reliability, and higher efficiency for each DG unit [27]. The main objective of this droop control is to safeguard a constant ratio of grid parameters (current, voltage, and power) in converters of the network for maintaining the regulated output power and voltage [28]. Refer to Figure 4, the converter output voltage ( $V_{Ci}$ ) can be formulated using Eq (1). In this paper, the droop controller uses the virtual (or droop) resistance ( $R_d$ ) multiplied with the output current  $I_i$  aiming to regulate the output voltage refer to its terminal reference values ( $V_{ref}$ ) as shown in Eq (1).

$$V_{Ci} = V_{ref} - R_{di} \cdot I_i \quad (1)$$

where,  $I_i$  is the converter current, and  $R_{di}$  is the virtual droop resistance, where  $i = 1, 2, 3, \dots, n$ . This  $i$  represents the possible number of converters in the network. Thus, refer to [28], since the droop control method owns the advantages of efficient DC voltage stabilization and fast power regulation, it has been widely used for DC voltage control in the IMG systems.

### 3.1. Analysis of circulating current and its suppression in the IMG network

In this section, the analysis of circulating current ( $I_C$ ) in the IMG network is done through the two parallel DCMGs with one DC-load refer to Figure 4. Here,  $I_1$  and  $I_2$  represent the converter output currents, while  $V_{OC1}$  and  $V_{OC2}$  converter output voltages from MG1 and MG2, while  $I_3$  and  $V_{OC3}$  represent the load current and load voltage respectively. Also  $R_1$ ,  $R_2$  and  $R_3$  are the aggregate equivalent resistances obtained by adding the virtual resistance ( $R_d$ ) with cable or real (physical) resistance ( $R_p$ ). The improved control strategies of the network under this study are achieved by controlling the  $R_{di}$ , aiming to decrease or increase the converter output voltages following their reference values. The role of converter-3 is to adjust the voltage according to the power demand on the load side, here is the DC load.

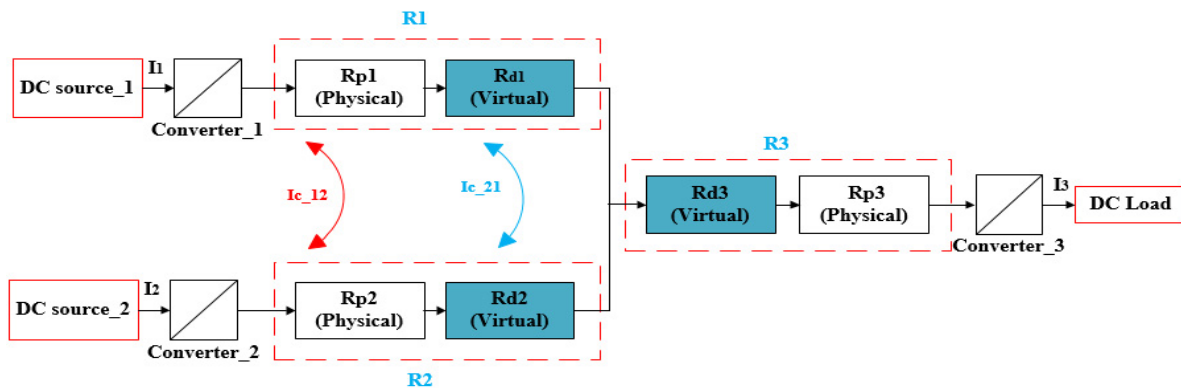


**Figure 4.** Circuit diagram of two interconnected DCMGs with droop controllers and load.

It was found in [29] that the  $I_C$  in the DCMG network could be minimized by inserting series resistance for controlling the voltage and current. Thus, the use of this series resistance is followed by additional power losses when two voltage sources in parallel are different. To improve this method, droop controllers shown in Figure 4 were designed with virtual resistances ( $R_d$ ) aiming to generate the balanced converter output voltages without additional power losses. This  $R_d$  can also stabilize and regulate the voltage levels in the DCMG network by adjusting it in response to the varying loads or other generating units. Since the voltage drop depends on the real resistance of the power line, there are no power losses associated with this droop control with the use of virtual resistance. However, if the resistance is high, the voltage of the buses of the network will deviate significantly from the rated voltage [10]. Using Kirchhoff's voltage law (KVL) refer to Figure 4, Eqs (2) and (3) are formulated, where  $V_{DC}$  is the voltage source from inverter.

$$V_{OC1} - (I_1 R_1 + I_3 R_3) = V_{DC1} \quad (2)$$

$$V_{OC2} - (I_2 R_2 + I_3 R_3) = V_{DC2} \quad (3)$$

The  $I_C$  (s) in the network can be expressed using Eqs (4) and (5). Here, the circulating currents  $I_{C12}$  from voltage source-1 to voltage source-2 and  $I_{C21}$  from voltage source-2 to voltage source-1 are of equal magnitude but with opposite directions.

$$I_{C12} = \frac{V_{OC1} - V_{OC2}}{R_{p1} + R_{p2}} = \frac{V_{OC1} - V_{OC2}}{2R_p} \quad (4)$$

$$I_{C21} = \frac{V_{OC2} - V_{OC1}}{R_1 + R_2} = \frac{V_{OC2} - V_{OC1}}{2R_p} \quad (5)$$

In this analysis,  $R_p$  in the IMG network is considered constant, and the equivalent value of the physical resistance for both MGs is  $2R_p$  as expressed in Eqs (4) and (5).

### 3.2. Control for voltage regulation

Referring to the analysis done above, it can be observed that due to the difference in cable resistance ( $R_p$ ) of the IMG, the converter output voltage could deviate, leading to the misbehavior of accuracy in current sharing among converters [30]. The voltage deviation ( $V_{error}$ ) can be calculated using Eq (6).

$$V_{error} = V_{ref} - V_{OC} \quad (6)$$

Effectively managing the voltage deviations in the IMG network, leads to operational stabilities and ensuring the reliability in power-sharing between IMG components [31]. If it is needed to change the voltage offset of the droop, for example, if the amount of power to be delivered by the converter is known, it will be necessary to calculate the current to be fed to that converter. This is also associated with the calculation of voltage drop in the droop resistance. This will lead to the choice of offset voltage needed for this control [32]. Here, the offset voltage will be equal to the terminal voltage plus the drop resistance multiplied by the current that can be fed [33]. Comparing the reference and output values of voltage, the voltage deviation in the local controller is calculated and then this voltage deviation is supplied to the corresponding proportion (P) controller. This P-controller deals with the regulation of output voltage from each converter by minimizing their corresponding voltage deviations. In summary, the main contribution of this paper is to provide an improved method for controlling an IMG for minimizing the voltage deviation between the reference voltage and the desired output voltage in the grid network, leading to proper load sharing, and reducing the circulating current and power loss. This method was also employed to ensure the stability of the IMG system in remote areas.

## 4. Methodology

In this paper, an IMG network is controlled to enable a group of individual autonomous off-grid networks to exchange power through the main DC bus, and are used in remote areas away from the national grid, where the power sources are from solar PV systems. Here, is the case study with the parameters described in Table 1, and these parameters were used for illustration purposes. During the analysis, the DESs are interconnected to the common DC bus using three (3) power converters with power cables interlinking the network parameters, which were considered during simulation using MATLAB/SIMULINK. In this paper, two (2) converters are considered as power supply, while the third converter (connected to the load) will be considered to draw power from these two. Also, the power ratings of the grid converters are assumed to vary from 200 to 1000 W according to the considered grid parameters of resistors, inductors, and load characteristics. After comparing the reference and output values of voltage, the voltage deviation in the local controller is calculated and then this voltage deviation, regarded as voltage error is fed to the corresponding P-controller to produce a regulated grid voltage. In this paper, it was assumed that current, voltage and power are from an IMG of 3-converters, but for validation of the results, this system can be extended to a network of n-converters with different types of DERs.

#### 4.1. Droop control design

The design of droop control could be achieved considering possible dynamics specified by the IMG network due to their effects on its working performance. In this type of control, the complete linear model with droop control parameters including droop gain, filter, feedback controllers, and reference parameters was considered. The feedback control system linked to its closed-loop droop controller is shown Figure 5. The significant role of this control method is to regulate the output voltage ( $V_{out}$ ) or  $V_{OC}$  so that it will match with  $V_{ref}$  at minimum voltage error ( $V_{error}$ ), resulting in the minimization of circulating currents. The regulated output voltage is provided through droop gain controller ( $K$ ) and the voltage deviation ( $V_{error}$ ) using Eqs (7) and (8).

$$V_{out} = V_{ref} - V_{error} \quad (7)$$

$$V_{loop} = K \times V_{error} \quad (8)$$

For an optimum controlled IMG, the value of  $V_{loop}$  must be the same as  $V_{out}$ . The droop resistance and droop gain are in line with the voltage droop control in the IMG, and it is noticed that the increase in  $R_d$  results in the decrease of  $K$  and vice versa. The regulation of voltage deviation will be based on the adjustment of this gain  $K$ . The virtual resistance ( $R_d$ ) was introduced in droop control of DCMG for modifying the behavior of the DERs voltage and improving the power-sharing and stability in the IMG network. This droop resistance is a crucial tool to manage the power flow and ensure efficient operation in the IMG systems. When the controlled output  $V_{loop}$  is not closer to  $V_{out}$ , this  $V_{loop}$  is fed back and compared with a reference voltage  $V_{ref}$  to generate  $V_{error}$ , which is also regulated using the droop gain controller ( $K$ ) until the  $V_{loop}$  will become closer to the  $V_{out}$ .

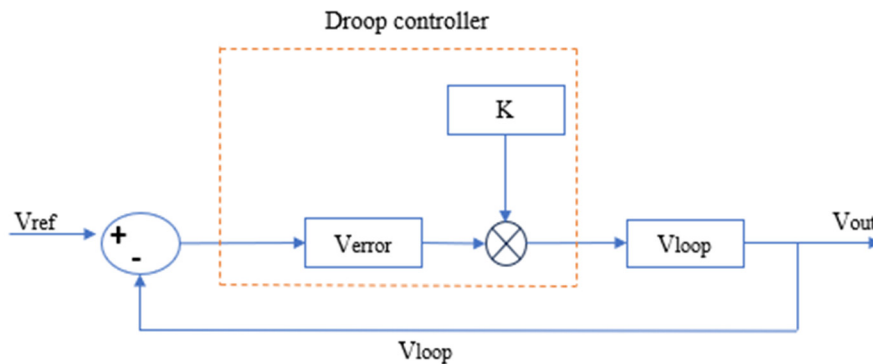


**Figure 5.** Proposed closed-loop droop controller.

In this work, the closed-loop droop control in the IMG network was achieved through the following steps: (i) Sensing: Voltage and current sensors are used to monitor the converter output parameters in each microgrid. (ii) Comparison: The sensed values will be compared with the reference values or desired set points. (iii) Error calculation: The error was detected by comparing actual values ( $V_{out}$ ) and reference set values ( $V_{ref}$ ) to minimize the  $V_{error}$ . (iv) Controller: The error is fed into the controller, and this will compute the needed control action. (v) Modulation: The control action will be used to modulate the switching signals of the converter by adjusting its output voltage. (vi) Feedback loop: The modulated output voltage is fed back to the system, continuously correcting any deviations and ensuring stable and accurate power-sharing.



#### 4.2. Microgrid components and control

In this work, the reference voltage values, line resistance, and line inductance of the paralleled power converters of the IMG network are shown in Table 1. In this study, the line parameters are assumed to be constant in the whole network, and all MGs are connected to the common bus at equal distances.

**Table 1.** Nominal IMG network parameters.

Parameters	Values
Reference voltage	100, 200 V
Line resistance	0.3 $\Omega$
Droop resistance ( $R_d$ )	0.5 $\Omega$
Line inductance	0.01 mH
Load set power	200; 400, 600, 800, 1000 W

### 5. Results and discussions

In this section, the IMG network was simulated and analyzed. This method is applied locally at each converter to improve network reliability by allowing power-sharing between network converters. The converter output current, voltage, and power under stability conditions are discussed. Also, Droop control of IMG parameters under constant load power and with change in load power is discussed. In these results, it was found that the regulated output voltage can be matched closer to the reference voltage with minimum voltage deviation through the use of droop controllers.

#### 5.1. Controlled converter output current, voltage, and power

In the IMG with droop control, the output current, voltage, and power depend on the specified control strategies that were employed. The control strategy used in this paper aims to regulate the current sharing between DERS and loads. Each source has the droop characteristic, determining how the output current will change with its corresponding output voltage. The droop control with the virtual resistance was employed to define a steady-state current and voltage regulation from each converter, and this defines the output data of each IMG converter.

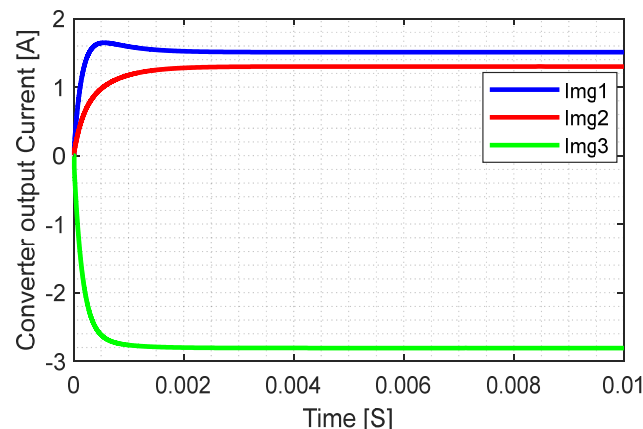


**Figure 6.** Output current from three converters when load power is set to 600 W.

The resulting currents corresponding to the three converters, i.e.,  $I_{mg1}$ ,  $I_{mg2}$ , and  $I_{mg3}$  are shown in Figure 6. Figure 7 shows the characteristics of the converter output voltage as V-Out1, V-Out2, V-Out3, and power in Figure 8 as PMG1, PMG2, and PMG3 with load power set to 600W respectively are shown. During this analysis, it was assumed that converter-1 and converter-2 work by supplying the power to converter-3, where finally this power from converter-3 will be delivered to the load. The droop control here helps to achieve stability and load sharing by regulating the output power, voltage, and current in line with the change in load demand. The specific control settings and droop slopes might be determined based on the MGs' design and requirements between the loads and the power sources involved. However, because DERs are all connected in parallel, the overall output power in the IMG might also be increased with increasing load demand, and each DER will contribute its power-sharing based on the droop control to allow the IMG network to respond to the variation in the variation of load conditions.

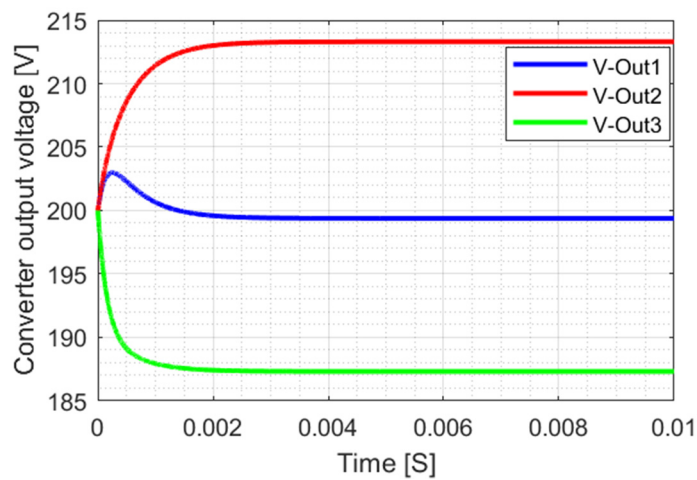


**Figure 7.** Output voltage from three converters when load power is set to 600 W.

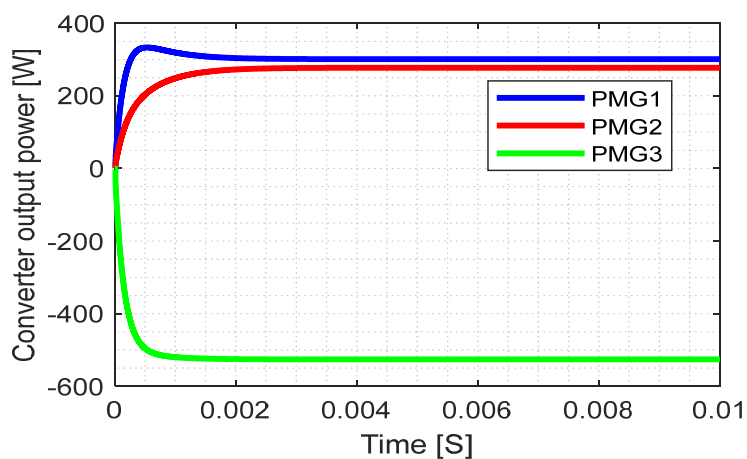


**Figure 8.** Output power from three converters when load power is set to 600 W.

In Figures 6–8, it is shown that the control of output powers, voltages, and currents provides the microgrid stability, resulting in stable converter power, where converter-3 is drawing power of 300.9 W

named PMG1 from converter-1 and converter-2 of 277.4 W named PMG2 resulting in the total power of 526.3 W named PMG3 as shown on Figure 8. The difference of 54 W from these two power converters with PMG3 is the power losses in this IMG network due to the line impedance. For better controlling the converter output voltage and power, droop controllers with virtual resistance are used instead of real resistances refer to the circuit diagram shown in Figure 4. The system of n-converters in an IMG network is said to be in steady state condition or stable when the power required by the loads is efficiently shared between these n-converters. Thus, in the case all converters are working under full load capacity, the network is said to be in steady state condition when all of these converters are delivering equal amounts of power. In this paper, refer to Figure 8, PMG1 and PMG2 are almost the same under steady-state conditions. Experimentally, a system with n-converters can be considered for validating the above results.

### 5.2. Regulated output current and voltage with droop gain controllers

In a parallel-connected DC microgrid, as the grid voltage increases, the corresponding output current will decrease according to its droop slope. Contrariwise, when the output voltage decreases, the output current will increase. The idea behind this is that as the load in the IMG network increases, the voltage will drop slightly, which causes the grid sources to increase their output current by sharing the additional load in the network. The regulated voltage and current are provided through the voltage and current inner loop shown in Figure 5. The I-V droop control characteristics using two droop gains  $K_1$  and  $K_2$  is represented in Figure 9 for two converters.

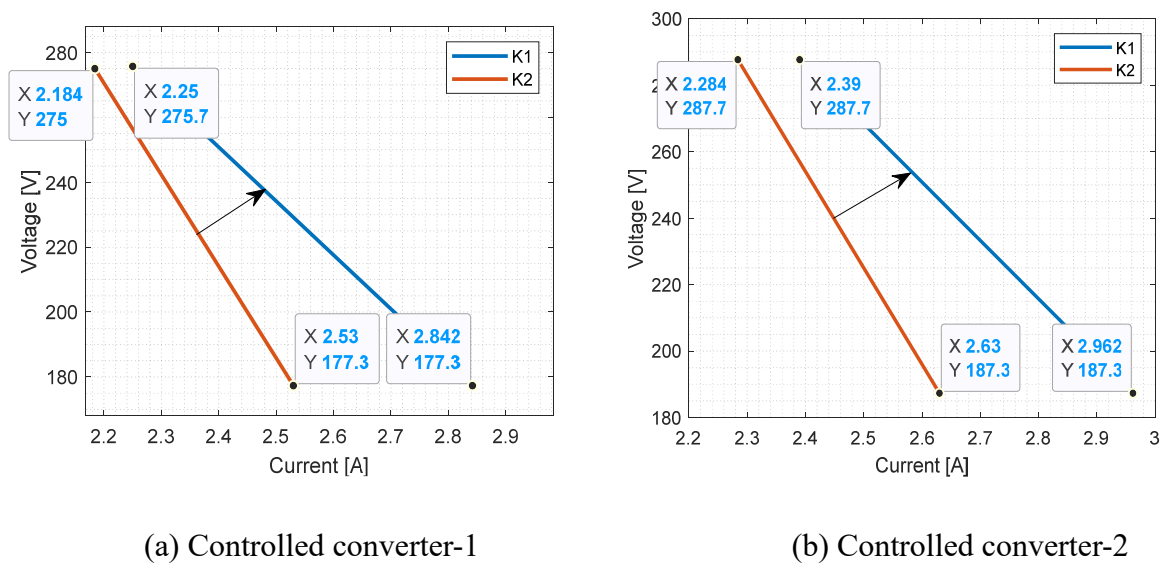


**Figure 9.** Output current regulation using droop control parameters ( $K_2$  and  $K_1$ ) at constant converter voltages of (a) Controlled converter-1 and (b) Controlled converter-2.

Referring to Figure 9 (a) and (b), it can be observed that the slope of the curve has changed, and the change makes the voltage change less for a given change of the current by comparing both currents  $I_2$  of 2.184 A and  $I_1$  of 2.25 A, while the voltage is changed from  $V_2$  of 270.6 V to  $V_1$  of 275.7 V. This condition is observed for both converter-1 and converter-2. It can be observed that the converter output voltage and current can be regulated using droop gain for each converter. In this work, it is reminded

that the droop control is used to achieve balanced power-sharing in the network, achieved by selecting a proportional controller and corresponding droop gains. It is noted that, for lower droop gains, this may result in mismatches among the output converter voltages and currents.

However, higher droop gains ( $K_2$  compared to  $K_1$ ) result in lower voltage drops at the output terminal of the grid converters, leading to a reduction in circulating currents. The converter output currents can also be controlled using  $K_1$  and  $K_2$  at the fixed output voltages, as seen in Figure 9 (a) for converter-1 and (b) for converter-2. It was observed that under the controlled converters, there is a current variation of 3.1% from  $K_2$  to  $K_1$  at a fixed voltage level of 275.7 V for converter-1, while for the converter-2, there is a current variation of 4.4% from  $K_2$  to  $K_1$  at a fixed voltage of 287.7 V. This results in the operating range of power from 448.6 to 602.1 W with a droop gain controller  $K_2$  and 503 to 620.3 W for  $K_1$  in the converter-1, i.e., the output voltage can be controlled through different values of droop gain controllers for improving the power-sharing. It can be noted that, with droop controllers, increasing the droop gains results in less voltage deviation between DERs.

### 5.3. Converter output voltage control using the feedback-controlled voltage

Another method of regulating the converter output voltage ( $V_{out}$ ) is done using the feedback-controlled voltage ( $V_{loop}$ ) by considering also the reference voltage ( $V_{ref}$ ). During this analysis, it is crucial to consider the output voltage ( $V_{out}$ ) resulting from the difference between the reference voltage ( $V_{ref}$ ) of 200 V) and the loop voltage, as shown in Figure 10. Here, the fixed reference power (initially at 300 W) was taken into consideration. Tracking the power references or load power set, involved the use of a conventional  $P$ -controller, where the power loop gets its corresponding reference input from the designed droop voltage loop. The output voltage and current are obtained using Eqs (9) and (10) respectively.

$$V_{out} = V_{ref} - K (I_{ref} - I_{out}) \quad (9)$$

$$I_{out} = \frac{V_{out}}{R_L} \quad (10)$$

where  $V_{out}$  is the controlled output voltage,  $K$  is the droop gain controller,  $R_L$  is the line resistance, while  $I_{out}$  is the output current. As shown in Figure 10 by considering one DC converter, the objective was achieved with a small value of voltage deviation ( $\Delta V$ ) of 0.35% from the controlled voltage ( $V_{loop}$ ) of 99.84 V and  $V_{out}$  of 100.2 V to the reference voltage value of 200 V. This small value of  $\Delta V$  is positive to the controlled network, and once this  $\Delta V$  becomes too high, the controllers are set again so that at the end a lower voltage deviation will be generated.

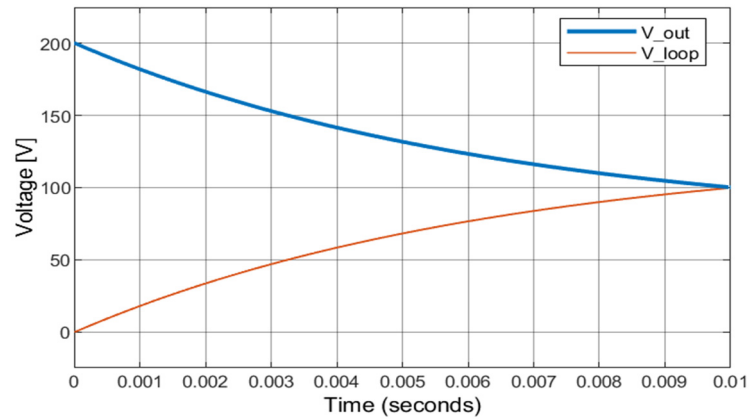


**Figure 10.** Output voltage and the controlled voltage responses at the load power set of 300 W.

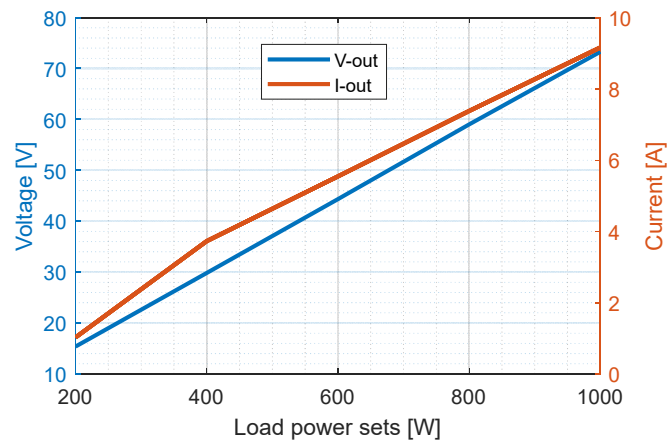


**Figure 11.** The output current and output voltage responses at different load power sets.

It can be observed that a mismatch in the voltages causes unequal current sharing within the network, resulting in additional power losses. It is in this regard that the droop control parameter varies the slope of output voltage characteristics to a closed value of the feedback control compared to reference converter voltage. To avoid large DC voltage deviation ( $\Delta V$ ), this controller needs a fast response time, as shown in Figure 11. For this case, the voltage deviation is minimized by regulating the droop gain ( $K$ ) so that  $V_{out}$  does not differ too much with the controlled voltage ( $V_{loop}$ ).

#### 5.4. Controlled output current, voltage, and power with constant loading conditions

From the droop-control of IMG, the output voltage from the respective DER is inversely proportional to the load current. In this case, with the increase in load current, the respective voltage will also decrease referring to the droop characteristic of the power source. In the IMG network with individual MGs operating in parallel, all power sources have similar droop characteristics, ensuring that the load is shared proportionally among them. Thus, the output voltage across each MG remains stable even when there is variation in load conditions. After regulating the output voltage through the droop control parameter ( $K_n$ ), it is observed that as the power sets increase, the corresponding voltage and current also proportionally increase.

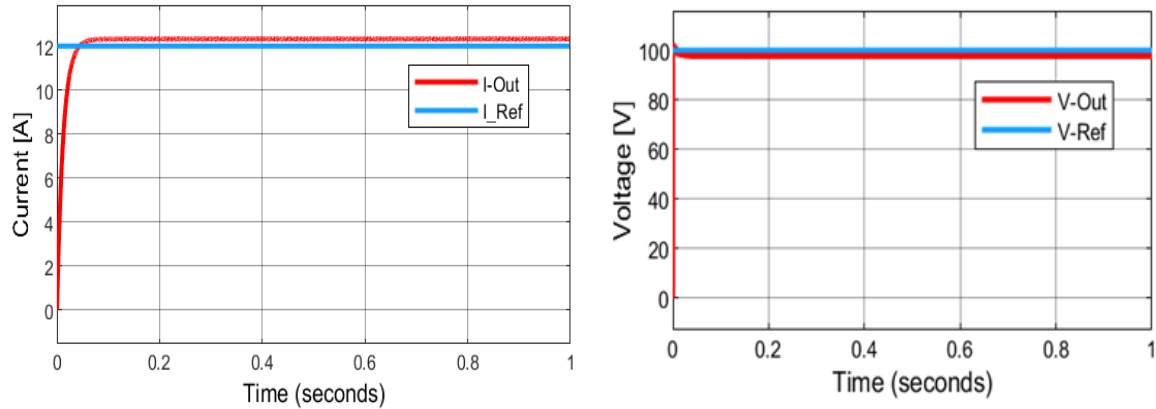


**Figure 12.** Regulated output current and voltage (for one converter) and their reference values.

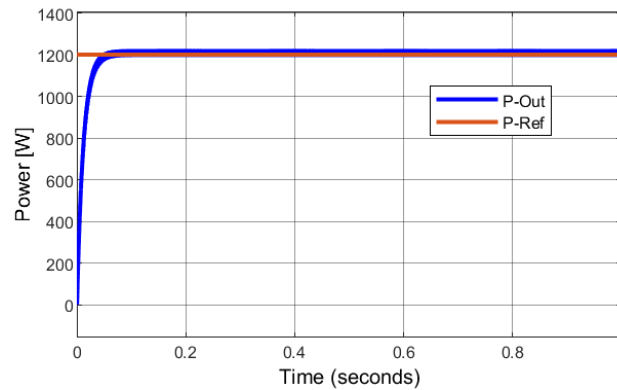


**Figure 13.** Power output with its corresponding reference value.

Therefore, the selection of the reference voltage and current values would depend also on the reference power of the grid for matching with the load demand. Thus, refer to Figure 12, both output current and voltage are regulated in a way that their values will not differ too much from their reference values. In this analysis, the regulated output voltage  $V_{out}$  of 98.8 V is achieved from the reference voltage ( $V_{ref}$ ) of 100 V, where the voltage deviation is reduced to a minimum value of 1.2 V. As a result of droop control, the output power ( $P_{out}$ ) shown in Figure 13 is also controlled, where this  $P_{out}$  becomes nearly equal to its reference value ( $P_{ref}$ ) of 1200 W.

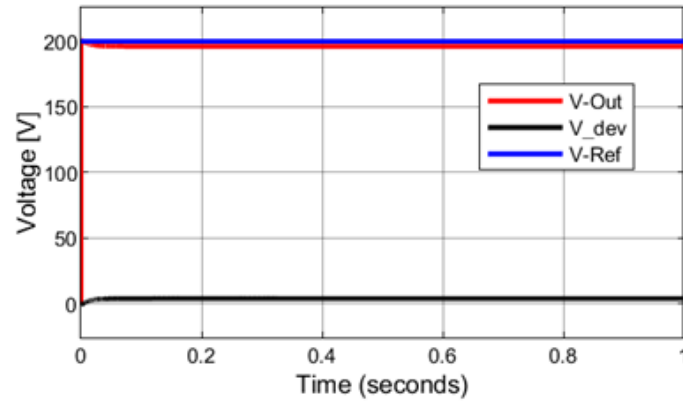


**Figure 14.** Regulated output voltage and voltage deviation at a reference voltage of 200 V.

To adjust the offset voltage of each grid converter, the voltage regulation will be achieved resulting in keeping the IMG system parameters, i.e., current, voltage, and power being operational closer to their reference ratings for having the network stability as shown in both Figures 12 and 13. The optimal offset voltage can be calculated based on the desired output voltage in addition to the production of droop resistance and the feeding current. Remarkably, the droop dynamics can be involved in the grid control stability in which, each grid converter will have reference values that match the load characteristics. Generally, droop set points of individual grid converter might be determined by finding optimum grid parameters.

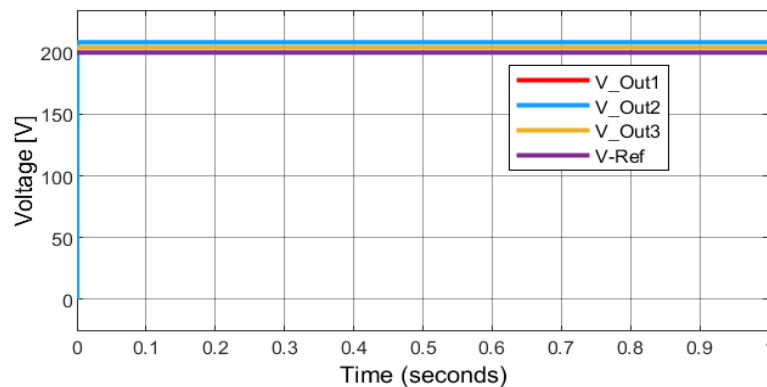


**Figure 15.** Controlled output voltages of three converters at 200 V of reference voltage.

In this paper, the objective of regulating the output voltage is achieved (refer to Figures 14 and 15). This is achieved through the minimization of the voltage deviation ( $V_{dev}$  or  $\Delta V$ ) closer to zero, as shown in Figure 14. Refer to Figure 15, as a result of voltage controllers, all output voltages (i.e., V-Out1, V-Out2, and V-Out3) from three network converters are closer to the reference voltage value of 200 V.

### 5.5. Droop control at different load power sets

This method of droop control in an IMG system helps the grid system to efficiently manage the power distribution with stable operation even during the change in load conditions. This method is also

a decentralized and flexible approach suitable for small and medium-scale DCMG systems. The purpose of this control method is to ensure the balanced load sharing among the DERs of an IMG while maintaining the grid network stability. Linked to the case study, different power loads have been used for testing the performance of this method. The results of the output power from the three converters and respective power losses are shown in Figure 16. To implement the proposed method for the droop controller, currents and voltage in the grid network must be measured and set to ensure an exact value of power set to avoid the effects of the load variations. Droop control in this work is used in the IMG, aiming for power load sharing and control of the output voltage. Here, the active load power could be shared among all DERs. The purpose of this control structure is to eliminate the voltage deviation to ensure equal power-sharing in the IMG network. In this analysis, the power supplied to the converter-3 is equivalent to the sum of both converter-1 and converter-2 subtracted by the corresponding power loss P-Loss.

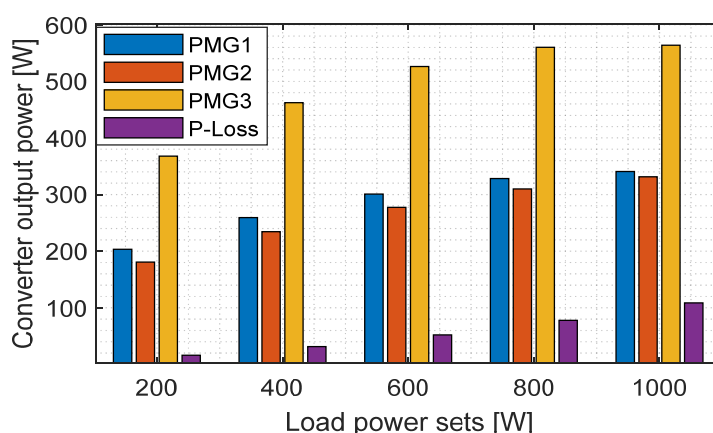


**Figure 16.** Converter output power from three converters with respective power losses using power sets of 200, 400, 600, 800, and 1000 W.

This power loss depends on the characteristics of the cable connecting all converters in the network. For example, as shown in Figure 16, at the load power set of 400 W the power from converter-1, and converter-2 are 259.3 and 234.4 W, respectively, while the power of converter-3 is 462.2 W with the corresponding power loss of 21.5 W. It was found that as the load power sets get increased, there are more power losses. Thus, the selection of load power during the modelling and simulation might be based on the possible number of converters in the network and the capacity of the power-generating units. It can be noted that during the implementation of this control method, the selection of the load power sets is an important parameter and there should be matching parameters between the supply and load power for optimizing the power losses in the designed IMG network.

### 5.6. Droop control of IMG parameters with change in load power

In the conditions of load power changing from 1 to 10 seconds, the results of the control approach are shown in Figures 17–19 for current sharing, voltage deviation, and power-sharing respectively. In this method, the change in voltage and current is subjected to the load conditions, i.e., the parameters at converter-3, and referring to the previous discussions, this converter is set to be a power consumer, while the remaining two are suppliers of converter-3. In this case, the droop controller is regulated



according to the change in both converter current and voltage errors, and this is done to meet the load demand, where the reference current  $I_{ref} = 5$  A refer to Figure 17. The higher current changes ( $I_{s3} = 34.3$  A at  $t = 7$  s and  $I_{s3} = 33.6$  A at  $t = 9$  s) were based on the high-power demand of  $P_3$  of 9.3 kW and  $P_3$  of 6.8 kW on the side of converter-3 (refer to Figure 19). Thus, with the droop controller, the characteristics of improved current sharing ( $I_{s1}$ ,  $I_{s2}$ , and  $I_{s3}$ ) among three converters are shown in Figure 17. Here, the waveforms for  $I_{s1}$  and  $I_{s2}$  have less overshoot, where they have peak and low values at the same time, and can be noted that the current from MG3 (or  $I_{s3}$ ) is the sum of both  $I_{s1}$  and  $I_{s2}$  refer to Figure 4.

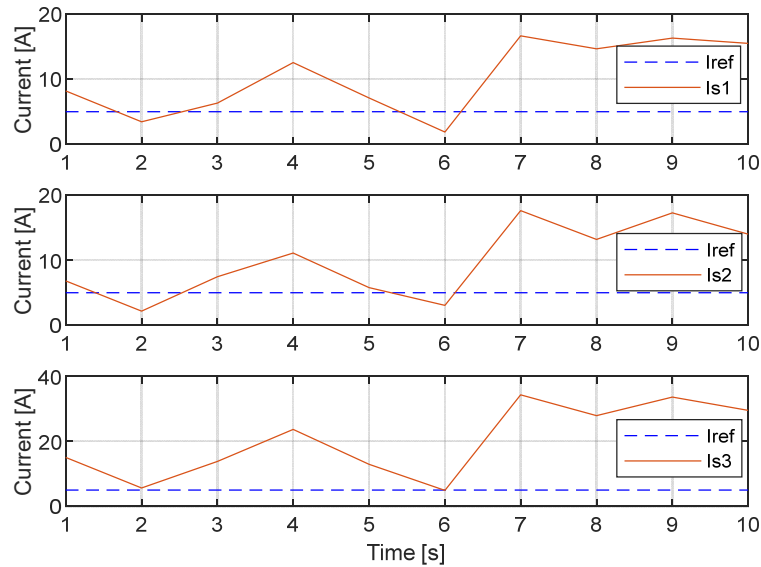


**Figure 17.** Current sharing control with its reference value under load changes.

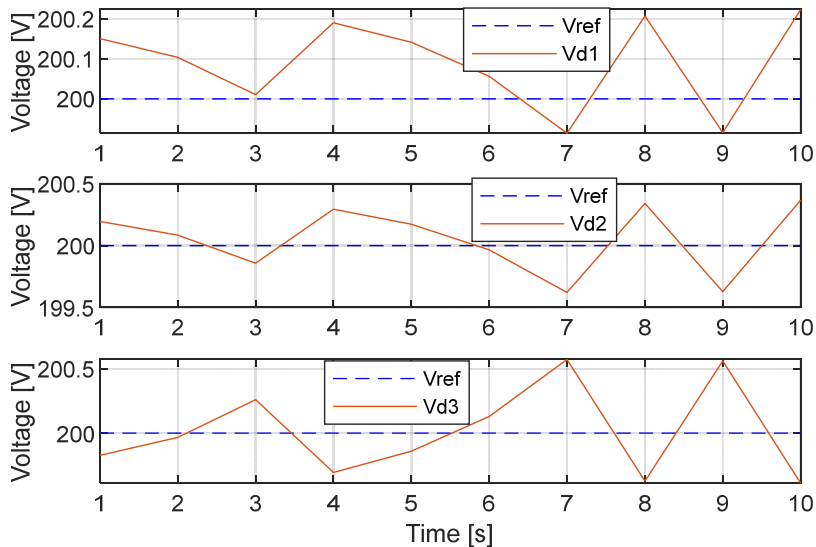


**Figure 18.** Voltage deviation control with reference value under load changes.

It was observed that each converter voltage converges to the grid reference voltage at a lower

voltage deviation as shown in Figure 18. In this analysis, the voltage deviation between the output voltage and reference values is less than 0.6 V, where the maximum values were found at  $t = 7$  s and  $t = 9$  s with the voltage variation in load voltage (i.e., converter-3) were found as 0.58 and 0.56 V, while the voltage deviation for both converter-1 and converter-2 remained below 0.5 V. This leads to efficient voltage regulation with minimum voltage variation, resulting in the stability of an IMG network. The results of controlling the voltage deviation among converters of the IMG network also affect the power-sharing among them, as shown in Figure 19. The proper power-sharing is observed on both converter-1 and converter-2 represented with  $P_1$  and  $P_2$ , respectively, where both are not facing high power variation.

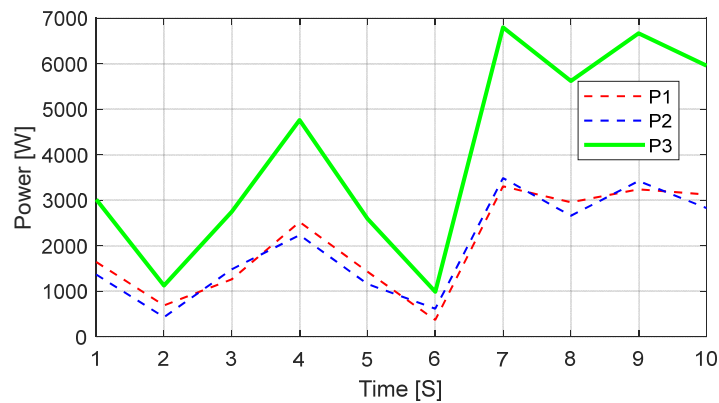


**Figure 19.** Output power control with its reference value under load changes.

In this paper,  $P_3$  is considered as load power defined by the sum of both  $P_1$  and  $P_2$ . Refer to the aforementioned analysis, this improved method for controlling the IMG using droop control is found to be an effective method that can be adopted for implementing the MG control with multiple DERs based on the regulation of current sharing and voltage deviation for achieving proper load sharing. Furthermore, the extension to the system of an IMG with  $n$ -converters could be implemented to validate the obtained results.

## 6. Conclusions

In this work, a droop controller for voltage regulation in an interconnected DC microgrid is analysed. The modelling and control systems are validated using MATLAB/SIMULINK, where related results and analysis are provided. Due to the intermitted nature of DERs, fluctuations in load demand from IMGs pose significant challenges in providing with regulated output voltage according to the load demand. The improved droop control method is adopted to obtain the system IMG stability at equal load sharing with low voltage deviation. It was found that through a droop controller, the output voltage of the converter can be controlled to be consistent with its reference value, where the main objective is to minimise the voltage deviation  $\Delta V$  to ensure the power-sharing in the IMG network, resulting in the suppression of circulating current. In this analysis, the minimum voltage deviation at the load side (converter-3) was found between 0.58 and 0.56 V, while the voltage deviation for both converter-1 and converter-2 remained below 0.5 V. It can be noted that this can lead to efficient voltage regulation, resulting in the stability of an IMG network. This is achieved through the droop

controllers installed in each MG and was analysed through the droop gain controllers for providing proper current sharing.

This control method can also be further extended by considering any n-parallel converters of the IMG system, where the control objective can be achieved with minimum power loss and current sharing to achieve network stability where the converter power is equally shared under steady-state conditions. It was observed that this improved method of controlling IMG using droop control proved to be an effective method to achieve MG control of multiple DERs based on the regulation of current sharing and voltage deviation for achieving proper load sharing. Generally, the results and analysis are based on the simulations, but beyond that, the results can be verified by implementation using real devices which will be the next step.

## Acknowledgements

The authors of this paper would like to acknowledge the sufficient support from the EPSRC under the Project EP/R030235/1 “RENGA: Resilient Electricity Networks for a Productive Grid Architecture” from the Imperial College of London, UK. Furthermore, the authors acknowledge important support from the African Center of Excellence Energy for Sustainable Development located at the University of Rwanda, College of Science and Technology (UR-CST).

## Conflict of interest

The authors declare no conflicts of interest.

## Use of AI tools declaration

The authors declare that they have not used Artificial Intelligence (AI) tools in the creation of this article.

## References

1. Dou CX, Zhang ZQ, Yue D, et al. (2017) Improved droop control based on virtual impedance and virtual power source in low-voltage microgrid. *IET Gener Transm Distrib* 11: 1046–1054. <https://doi.org/10.1049/iet-gtd.2016.1492>
2. Rodriguez-Bernuz JM, Junyent-Ferré A, Xiang X (2020) Optimal droop offset adjustments for accurate energy trading in rural DC mini-grid clusters. *2020 International Conference on Smart Grids and Energy Systems (SGES)*, Perth, Australia, 453–458. <https://doi.org/10.1109/SGES51519.2020.00086>
3. Hategekimana P, Junyent-Ferré A, Rodriguez-Bernuz JM, et al. (2020) Assessment of feasible DC microgrid network topologies for rural electrification in Rwanda: Studying the kagoma village. *2020 International Conference on Smart Grids and Energy Systems (SGES)*, Perth, Australia, 854–859. <https://doi.org/10.1109/SGES51519.2020.00157>
4. Anand Abhishek SK, Aashish R, Sachin D, et al. (2020) Review of hierarchical control strategies for DC microgrid. *IET Renewable Power Gener* 14: 1631–1640. <https://doi.org/10.1049/iet-rpg.2019.1136>

5. Mohamed MA, Abdullah H, Al-sumaiti A, et al. (2020) Towards energy management negotiation between distributed AC/DC networks. <https://doi.org/10.1109/ACCESS.2020.3040503>
6. Gorijeevaram Reddy PK, Dasarathan S, Krishnasamy V (2021) Investigation of adaptive droop control applied to low-voltage DC microgrid. *Energies* 14: 1–20. <https://doi.org/10.3390/en14175356>
7. Hai NT, Kim KH (2016) An adaptive virtual impedance based droop control scheme for parallel inverter operation in low voltage microgrid. *Int J Power Electron Drive Syst* 7: 1309–1319. <https://doi.org/10.11591/ijpeds.v7i4.pp1309-1319>
8. Kala B, Raju A, Varun J, et al. (2018) Circulating current minimization in low-voltage DC microgrid based on droop control strategy. *Int J Res Anal Rev* 5: 577–582.
9. Rawaa A (2022) Voltage control and power sharing in DC microgrids (DCMG). *CASE West Reserv Univ*, 1–69.
10. Rashad M, Raouf U, Siddique N, et al. (2021) Mitigation of circulating currents for parallel connected sources in a standalone DC microgrid. *Eng Proc* 12: 4–9. <https://doi.org/10.3390/engproc2021012031>
11. Tameemi Z, Lie T, Foo G, et al. (2022) Optimal coordinated control strategy of clustered DC microgrids under load-generation uncertainties based on GWO. *Electronics* 11: 1244. <https://doi.org/10.3390/electronics11081244>
12. Tameemi Z, Lie T, Foo G, et al. (2021) Control strategies of DC microgrids cluster: A comprehensive review. *Energies* 14: 7569. <https://doi.org/10.3390/en14227569>
13. Nascimento R, Ramos F, Pinheiro A, et al. (2022) Case study of backup application with energy storage in microgrids. *Energies* 15: 9514. <https://doi.org/10.3390/en15249514>
14. Lexuan M, Qobad S, Giancarlo F, et al. (2017) Review on control of DC microgrids and multiple microgrid clusters. *IEEE J Emerg Sel Top Power Electron* 5: 928–948. <https://doi.org/10.1109/JESTPE.2017.2690219>
15. Yang H, Zhang Y, Wang P (2021) Flexible interconnection of DC microgrid cluster based on isolated bidirectional DC-DC converter. *Syst Sci Control Eng* 9: 641–650. <https://doi.org/10.1080/21642583.2021.1975322>
16. Fathi M, Bevrani H (2017) Regulating power management in interconnected microgrids. *J Renewable Sustainable Energy* 9: 055502. <https://doi.org/10.1063/1.5003003>
17. Islam M, Yang F, Amin M (2021) Control and optimisation of networked microgrids: A review. *IET Renewable Power Gener* 15: 1133–1148. <https://doi.org/10.1049/rpg2.12111>
18. Han Y, Pu Y, Li Q, et al. (2019) Coordinated power control with virtual inertia for fuel cell-based DC microgrids cluster. *Int J Hydrogen Energy* 44: 25207–25220. <https://doi.org/10.1016/j.ijhydene.2019.06.128>
19. Ullah S, Haidar A, Hoole P, et al. (2020) The current state of distributed renewable generation, challenges of interconnection and opportunities for energy conversion based DC microgrids. *J Clean Prod* 273: 122777. <https://doi.org/10.1016/j.jclepro.2020.122777>
20. Hategekimana P, Junyent-Ferré A, Rodriguez-Bernuz JM, et al. (2022) Fault detecting and isolating schemes in a low-voltage DC microgrid network from a remote village. *Energies* 15: 1–16. <https://doi.org/10.3390/en15124460>
21. Chen J, Alnowibet K, Annuk A, et al. (2021) An effective distributed approach based machine learning for energy negotiation in networked microgrids. *Energy Strateg Rev* 38: 100760. <https://doi.org/10.1016/j.esr.2021.100760>

22. Tepe IF (2022) A review of control strategies and metaheuristic algorithms used in DC microgrids. *Int J Renewable Energy Res* 12: 799–818.
23. Peyghami S, Mokhtari H, Blaabjerg F (2017) Hierarchical power sharing control in DC microgrids. *Microgrid*, 63–100. <https://doi.org/10.1016/B978-0-08-101753-1.00003-6>
24. Li Z, Shahidehpour M, Aminifar F, et al. (2017) Networked microgrids for enhancing the power system resilience. *Proc IEEE* 105: 1289–1310. <https://doi.org/10.1109/JPROC.2017.2685558>
25. Lu X, Guerrero JM, Sun K, et al. (2014) An improved droop control method for DC microgrids based on low bandwidth communication with dc bus voltage restoration and enhanced current sharing accuracy. *IEEE Trans Power Electron* 29: 1800–1812. <https://doi.org/10.1109/TPEL.2013.2266419>
26. Zammit D (2022) Control of DC microgrids for distributed generation including energy storage. *Univ Malta (PhD thesis)*, 1–255.
27. Aluko A, Swanson A, Jarvis L (2022) Modeling and stability analysis of distributed secondary control scheme for stand-alone DC microgrid applications. *Energies* 15: 1–18. <https://doi.org/10.3390/en15155411>
28. Li B, Li Q, Wang Y, et al. (2020) A novel method to determine droop coefficients of DC voltage control for VSC-MTDC system. *IEEE Trans Power Deliv* 35: 2196–2211. <https://doi.org/10.1109/TPWRD.2019.2963447>
29. Siva Sankar BRKK, Valli VS (2020) A droop control strategy for minimization of circulating current in low-voltage DC micro grid. *Pramana Res J* 10: 145–153.
30. Zhang L, Chen K, Chi S, et al. (2019) The hierarchical control algorithm for DC microgrid. *Energies* 12: 2995. <https://doi.org/10.3390/en12152995>
31. Mokhtar M, Marei MI, El-sattar AA, et al. (2018) Improved current sharing techniques for DC microgrids. *Electr Power Components Syst* 46: 757–767. <https://doi.org/10.1080/15325008.2018.1512176>
32. Panda M, Bhaskar DV, Maity T (2022) A fuzzy-based coordinated power management strategy for voltage regulation and state-of-charge balancing in multiple subgrid-based DC microgrid. *Int Trans Electr Energy Syst* 2022. <https://doi.org/10.1155/2022/1288985>
33. Cucuzzella ASM, Trip S, De Persis C, et al. (2019) A robust consensus algorithm for current sharing and voltage regulation in DC microgrids. *IEEE Trans Control Syst Technol* 27: 1583–1595. <https://doi.org/10.1109/TCST.2018.2834878>



AIMS Press

© 2024 the Author(s), licensee AIMS Press. This is an open access article distributed under the terms of the Creative Commons Attribution License (<http://creativecommons.org/licenses/by/4.0>)